

# New Results for Digital Beamforming in MRI

Emad Ebbini<sup>1</sup>, Lance Delabarre<sup>2</sup>, J. Thomas Vaughan<sup>3</sup>, and Anand Gopinath<sup>4</sup>

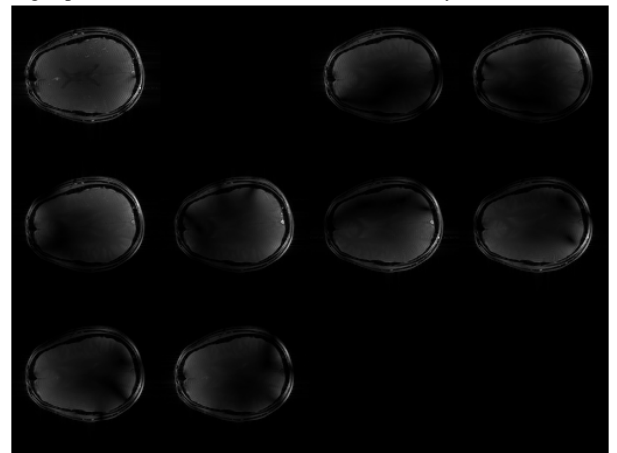
<sup>1</sup>University of Minnesota, Minneapolis, Minnesota, United States, <sup>2</sup>Radiology, University of Minnesota, Minneapolis, Minnesota, United States, <sup>3</sup>CMRR, Radiology, University of Minnesota, Minneapolis, Minnesota, United States, <sup>4</sup>ECE, University of Minnesota, Minneapolis, Minnesota, United States

## Introduction

Earlier digital beamforming methods employed in MRI largely focused on the correlation matrix to improve the signal to noise ratio. In addition, the use of matched filtering was shown to further improve the signal to noise in multi-coil MRI without a-priori knowledge of individual coil sensitivities or noise correlation structure. A number of studies have shown that such methods approached the performance of the standard sum of squares image reconstruction methods. At higher frequencies, however, the coil sensitivity maps become increasingly important and should be taken into account in optimal reconstruction. We have previously proposed a digital beamforming algorithm that incorporated the knowledge of the transmit-receive coil array geometry in deriving a propagation operator,  $\mathbf{H}$ , with elements,  $H(n,m)$  obtained from the complex of the  $n$ th array element at the  $m$ th observation (in image space) point. For a discrete set of observation points,  $M$ , the propagation operator is a matrix of size  $M \times N$ , where  $N$  is the number of coils used. The observation points can be selected based on a variety of criteria, but they typically they serve as a set of control points for an array pattern synthesis problem to optimize the array sensitivity in transmit and/or receive at these points. For example, this may be used to counter the effect of field heterogeneity by controlling the relative sensitivity at the different control points based on a priori knowledge of the field distribution. Given the complex field vector  $\mathbf{f}$  at the observation (control) points, it is possible to find a *pseudoinverse operator*,  $\mathbf{H}^\dagger$ , to solve for the complex weights of the array excitation,  $\mathbf{u}$ , to approximate  $\mathbf{f}$  at the control points under some optimality criterion. For example, the standard Moore-Penrose pseudo inverse provides a minimum-norm least squares approximation. Other criteria could be invoked is warranted by the problem requirements, but the results below are obtained with this pseudoinverse. This approach allows for the use of advanced digital beamforming methods with optimized sensitivity at select locations in the image space. More generally, it allows for forming images by compounding a number of reconstructions with different sensitivity functions. In this paper, we present 7-T MRI images obtained by compounding from compounding transmit-receive synthetic aperture beamforming (SA) reconstructions from complex image-space data from a 8-coil transmit-receive array.

## Data Collection and Standard RSS Reconstruction

MR data was collected from an 8-coil transmit-receive array with a diameter of 265 mm with the elements uniformly distributed (45° angular spacing). The subject was a healthy volunteer and the data was collected in sets with 1) All transmitter elements on with 45° phase rotation (Xmit#1), 2) All transmitter elements off (Xmit#2), and 3) Transmitter element  $i$  on ( $i = 1, 2, \dots, 8$ , Xmit#3,4, ..., 10). In all cases, root of sum of squares (RSS) images were formed from the 8-receive channels, i.e. 10 images were formed by simply taking the square root of the sum of squared values of the 8 complex data corresponding to the receivers. The images are shown in the figure to the right for reference. It should be noted that the data was collected from a low flip angle (45°) excitation with TR/TE = 40/4.08 ms with 250x250 mm<sup>2</sup> FOV and 128x128 pixel slice. A montage of the RSS images (Xmit#1 ... Xmit#10 from left to right, top to bottom) is shown to the right for the reference. One can see that all the images are generally low contrast (ventricles barely visible on all images). One can see that the RSS reconstruction from the individual element transmission exhibits dark regions reflecting the nonuniform element sensitivities.



## SA Beamforming and Compounding

The complex image data obtained from the 8 receive elements for each of the individual element transmits (Xmit 3 – 10) were used in a synthetic aperture beamforming and compounding scheme that can be described by the following equation:

$$I(x, y) = \sum_{l=1}^{N_g} C_l(x, y) \sum_{i=1}^8 \sum_{j=1}^8 u_i^T(x_l, y_l) u_j^R(x_l, y_l) I_{ij}(x, y) \quad \text{where the complex weights, } u_i^T \text{ and } u_j^R \text{ are obtained using the pseudoinverse}$$

optimal synthesis to focus at  $(x_l, y_l)$ . In this paper, the set of focal points were distributed on a 9x9 rectangular grid with 10 mm spacing in lateral and sagittal and coronal directions (centered at 0,0). This choice reflects the extent of the array point spread function (half-power width ~30 mm). The compounding function,  $C_l(x, y)$ , was computed from the psf at focusing point  $(x_l, y_l)$  to equalize the array focusing gain according to:

$$C_l(x, y) = \frac{psf(x, y; x_l, y_l) Mask(x, y)}{|psf(x, y; x_l, y_l)|^2 + \gamma}$$

which is shown in the figure to right, together with the array psf at the far most grid point in the sagittal and coronal direction. One can observe that the array psf does not change significantly from the psf at the array center, which is a Bessel function. The equalizing nature of the compounding function is also clear. In the above equation,  $\gamma$  is a regularization parameter and  $Mask(x,y)$  is a mask representing the region of support in the image space.

Finally, we show the resulting synthetic-aperture beamforming compounding image obtained using the algorithm described above. One can observe a significant increase in contrast and the appearance of several anatomical features that were hardly visible on the RSS images shown above.

Results from *in vivo* human brain images demonstrate significant improvement in contrast compared to RSS processing.

## Conclusions

A propagation operator from an 8-element array of transmit-receive coils to a set of control points in the image space was derived and used to obtain optimal phase and amplitude distribution for full synthetic-aperture beamforming and compounding. Results from *in vivo* human brain images demonstrate significant improvement in contrast compared to RSS processing.

## References:

- [1] J. T. Vaughan, et al, MRM1994, 32:206-218. [2] G. Adriany et al, MRM,2005, 53: 434-445. [3] P. B. Roemer, et al., MRM 1990,16:682-690. [4] D. O. Walsh, et al, MRM 2000, 43:192-225. [5] A. Gopinath, et al, ISMSRM Annual Meeting, 2012

